Biochimica et Biophysica Acta 933 (1988) 249–257
Elsevier

BBA 42755

Spectroscopic characterization of the acceptor state Q_A^- and the donor state S2 of Photosystem II of spinach in the blue, red and near-infrared

Bruno R. Velthuys

Laboratoire de Photosynthese, ER 307, CNRS, Gif-sur-Yvette (France)

(Received 30 November 1987)

Key words: Photosystem II; Electrochromic bandshift; Reaction center pheophytin; Scattering; (Spinach)

With Photosystem II particles prepared from spinach, partial difference spectra were measured of the primary bound plastoquinone Q_A and of the donor state S2. Extinction coefficients were estimated by comparison with the absorption change of a redox-active dye, *N,N,N′,N′*-tetramethyl-*p*-phenylenediamine. The spectrum of $Q_A^- - Q_A$ was better resolved than in earlier studies (Van Gorkom, H.J. (1974) Biochim. Biophys. Acta 347, 439–442; Schatz, G.H. and Van Gorkom, H.J. (1985) Biochim. Biophys. Acta 810, 283–294; Dekker, J.P. (1985) Thesis, University of Leiden) and is seen to be largely composed of shifts of two pigment bands in opposite directions, presumably a pheophytin red shift and a chlorophyll blue shift, as in bacterial reaction centers (Clayton, R.K. and Straley, S.C. (1972) Biophys. J. 12, 1221–1234). The spectrum of S2–S1 in the red suggests blue shifts of two chlorophyll bands. It resembles, but is not identical to, the S2–S1 spectrum earlier reported for Photosystem II of *Synechococcus* (Saygin, O. and Witt, H.T. (1985) FEBS Lett. 187, 224–226). Earlier measurements of S2-associated absorbance in the near-infrared (Dismukes, G.C. and Mathis, P. (1984) FEBS Lett. 178, 51–54) are not confirmed. The observed changes in this range are probably largely scattering changes. This conclusion is reached on the basis of theoretical considerations

Introduction

Photosystem II (PS II) oxidizes water and reduces plastoquinone (for a review, see Ref. 1). One complete turnover of PS II requires four successive photoreactions. A short flash of light induces only a single photoreaction; it leads to the semireduction of a bound plastoquinone and the oxidation of an endogenous component of PS II. The oxidation of the endogenous component is usually described in formal terms, as a conversion of 'PS II oxidation state S1' to 'PS II oxidation state S2'.

It has been shown that the conversion of the S1 to S2 is detectable by means of absorbance measurements [2–7]. In the work reported here, I have re-determined parts of the S2 – S1 spectrum in the visible and near-infrared spectral range. I also remeasured parts of the absorbance spectrum associated with the semireduction of the bound plastoquinone, Q_A. My objective was to verify the published data, and to try to obtain greater accuracy than obtained previously. I used a similar method as that used by Hiayama and Ke in their measurement of a Photosystem I component, P-700 [10]: the redox reactions were coupled to those of a dye, *N,N,N′,N′*-tetramethyl-*p*-phenylenediamine (TMPD).

Abbreviations: PS II, Photosystem II; IR, infrared; TMPD, *N,N,N′,N′*-tetramethyl-*p*-phenylenediamine; DCMU, 3-(3,4-dichlorophenyl)-1,1-dimethylurea.

Correspondence: B.R. Velthuys, Laboratoire de Photosynthèse, ER 307, CNRS, F-91198 Gif-sur-Yvette Cedex, France.

Materials and Methods

PS II particles were prepared from spinach according to Bertold, Babcock and Yocum [11], stored at −20 °C at 5 mM chlorophyll in medium A (sucrose 0.4 M, NaCl 10 mM and MES-NaOH 25–13 mM, pH 6.5) and 35% ethylene glycol, and used over a period of several months. Inactivated (Mn-extracted) particles were prepared by incubating PS II particles in medium A with 2 mM NH_2OH and 1 g/ml Chelex resin, followed by centrifugation and resuspension in medium A.

Flash-induced absorbance changes were measured with a home-built instrument. The measuring light was obtained from a Cary 14PM monochromator. Its intensity, in a split-beam arrangement (only one of the beams passing through the cuvette), was measured with EG&G HUV-4000B photodiodes, which were protected from actinic light by blue filters (2 × Corning CS 4-96) or red filters (Corning CS 2-58 and 2-59). The measuring light was admitted through a shutter (Vincent Uniblitz 225). A few milliseconds after opening this shutter, each photodiode signal was automatically nulled by applying off-sets produced by home-built, low-drift Sample and Hold (S&H) amplifiers (held in Hold mode except when nulling; as in Ref. 12). The remainders were amplified and normalized by being passed through Analog devices AD534 analog dividers, using the S&H signals as divisors. The difference between the two signals was recorded on a home-built transient recorder. Actinic flashes were obtained from an EG&G FX101 flash tube, which was fed with 1 μF at 1300 V, and passed through either red or blue filters (so as to be invisible to the photodetectors). The instrument was piloted by a microcomputer (Tandy Color Computer). The same computer, programmed in assembly language, also provided the functions of signal averaging, curve fitting, etc.

The standard reaction mixture contained medium A (pH 6.5) plus 500 μM TMPD, 40 μM ferricyanide (producing 40 μM $TMPD^+$), 1 μM DCMU, and PS II particles at 50 μg chlorophyll/ml or 100 μg/ml (the latter only with measurements in the near-IR). To prevent oxidation of TMPD by oxygen, the experiments were performed with evacuated solutions, under a nitrogen atmosphere. All experiments were carried out at room temperature (17–27 °C). The optical pathlength of the cuvette was 2 mm. The spectral bandwidth was 6 nm in the blue, 3 nm in the red and 10 nm in the near-IR. The mixture in the cuvette was stirred every 5 min (to counter a tendency of the particles to aggregate) and replaced every 30 min. Measurements were repeated with 1-min intervals. Each data point of Figs. 2 and 3 is the average result of 30–50 (Fig. 2) or 100–200 (Fig. 3) measurements. The error bar given for one point of each panel is typical for the plus-and-minus standard deviation of all data of a panel. The standard deviation was essentially zero in Fig. 2B.

Results

Conditions and estimation procedures

Fig. 1 shows some typical traces obtained in this study. For reasons that will be explained in the next paragraph, traces A–D (but not E) were constructed using two different lengths of dark periods before the flash: recordings at short dark periods (2 s) were subtracted from recordings at long dark-periods (60 s). All measurements were

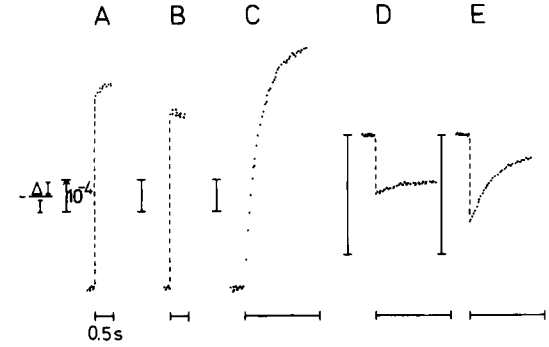

Fig. 1. Flash-induced absorbance changes in the presence of TMPD and DCMU. (A) Mn-extracted particles; 570 nm. The trace shown represents the difference between traces that were obtained with 1 min dark before the flash and with 2 s dark before the flash; it is the average of eight such pairs. (B) Same as A, but at 420 nm. (C) Same as A, but with non-extracted particles. (D) Same as C, but at 700 nm. (E) Non-extracted particles; 700 nm; 2 s dark before the flash. All traces: TMPD, 500 μM; ferricyanide, 40 μM; DCMU, 1 μM; pH, 6.5; chlorophyll, 50 μg/ml; optical pathlength, 2 mm; vertical units, $\Delta I/I$ of 10^{-4} per length indicated; horizontal units, 0.5 s per length indicated.

performed in the presence of DCMU, TMPD and $TMPD^+$. These conditions were also examined earlier [13,14]. The illumination of a dark-adapted sample by a flash leads to the reduction of Q_A and the oxidation of another PS II component. The nature of this oxidized component differs for Mn-extracted and non-extracted particles. When Mn-extracted particles are used (Fig. 1A and B), the oxidized component is a substance called 'Z'. This Z^+ rapidly reacts with TMPD [13,14], so that a few ms after the flash the PS II centers differ from the dark-adapted state only by containing Q_A^- instead of Q_A. The amount of Q_A^- is equal to the amount of TMPD that was oxidized. The latter is accurately measured at 570 nm, where $TMPD^+$ absorbs strongly. The absorbance changes due to Q_A reduction are negligible at this wavelength [4]. In contrast, $TMPD^+$ absorbs only weakly from approx. 410 to approx. 460 and above approx. 650 nm, and absorbance changes as in Fig. 1B (420 nm) are, therefore, largely due to Q_A reduction. When non-extracted particles are used (Fig. 1C and D), the flash illumination leads again to reduction of Q_A and oxidation of Z, but Z^+ now oxidizes a Mn-containing component, converting it from state S1 to state S2 (in comparable material, chloroplasts, this happens with a half-time of about 70 μs [3]). The Mn component in turn oxidizes TMPD, but this reaction occurs in the 100 ms time range and is easily monitored. At 570 nm (Fig. 1C), absorbance due to the S2 decay is negligible [4]. In contrast, at wavelengths where $TMPD^+$ absorbance is small, kinetically resolved absorbance changes are largely due to differential extinction of S1 and S2.

Rather than single flashes, sequences of four flashes were given, using a flash spacing of 2 s. This was done to correct for PS I contributions; the PS II preparation contains some PS I as a contaminant. As is seen, e.g., by monitoring at 700 nm, the P-700 component of PS I is oxidized by each flash and is rereduced by TMPD with a half-time of about 100 ms (Fig. 1E). However, all flashes except the first cause little PS II turnover: because of the presence of the inhibitor DCMU, Q_A^- remains largely reduced between flashes. It is oxidized by $TMPD^+$ with a half-time of approx. 6 s (not shown). To remove the PS I contribution from the first trace of a sequence, one of the later traces was subtracted from it (actually, the average of the third and the fourth trace was used for this purpose). The results of this manipulation were retained for analysis.

The Q_A^- minus Q_A extinction coefficients were calculated from the data obtained with Mn-extracted particles, by simple comparison of amplitudes at 200 ms after the flash: the amplitude at each wavelength, λ, was divided by the amplitude at 570 nm, multiplied by the extinction coefficient of $TMPD^+$ at 570 nm, and the resulting value was corrected for the extinction coefficient of $TMPD^+$ at wavelength λ. The extinction coefficient of $TMPD^+$ at 570 nm was taken to be 11 per $mM \cdot cm^{-1}$ [10,15]. The coefficients at other wavelengths were based on this value and a $TMPD^+$ minus TMPD difference spectrum that was measured by using oxygen as the oxidant. The S2 minus S1 extinction coefficients were calculated from the data with non-extracted particles, as follows: The section of the trace between 15 ms and 200 ms after the flash was fitted as a sum of two components: (1) the same section at 570 nm, multiplied by some factor (the parameter to be optimized), and (2) a remainder deviating sum-of-squares minimally from a horizontal line. The factor thus obtained was multiplied by the extinction coefficient of $TMPD^+$ at 570 nm; the extinction coefficient of $TMPD^+$ at the wavelength of measurement was subtracted. The 570 trace, used as a standard in the manner described, was frequently remeasured so that day-to-day variations in conditions (e.g., due to degradation of the particle preparation) did not degrade accuracy. A final correction was somewhat approximate. The decay of S2 under the conditions used is largely due to reduction by TMPD, but not exclusively. A competing pathway is recombination with Q_A^-. The half-time of this reaction was about 1 s [16]. The half-time of the reaction with TMPD was about 65 ms (estimated from traces as Fig. 1C). To correct for this competition, the numbers as calculated above were multiplied by 0.94, and 0.06 times the extinction coefficient of $Q_A^- - Q_A$ was subtracted.

The Q_A^- minus Q_A difference spectrum

The Q_A^- minus Q_A spectra in the blue and in the red are shown in Fig. 2A and B. The correc-

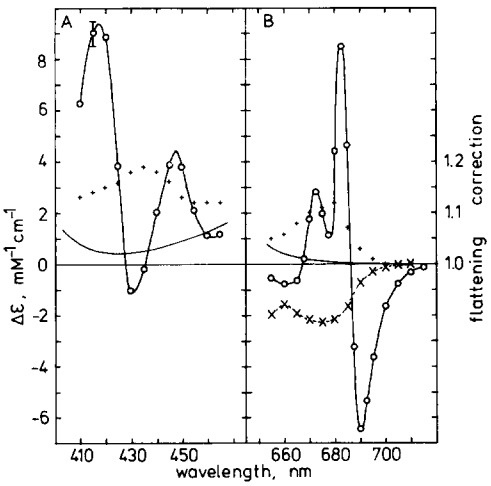

Fig. 2. Absorbance difference spectra of reduced minus oxidized Q_A (○). (A) 415–465 nm. Experimental conditions were the same as those described in Fig. 1A and B. Amplitudes at 200 ms were plotted against wavelength after correction for oxidation of TMPD. The spectrum of the latter is also shown (thin continuous line). The data were normalized against the absorbance change due to TMPD at 570 nm, taking $\Delta\varepsilon(TMPD^+ - TMPD, 570\ nm) = 11\ mM^{-1}\cdot cm^{-1}$ and $\Delta\varepsilon(Q_A^- - Q_A, 570\ nm) = 0$. To correct for 'particle flattening' (see text), the plotted data should be multiplied by the indicated correction factors (+), which were taken from Ref. 20. (B) 655–715 nm. Same as A, but 2 mM DNB was added to suppress contaminating fluorescence changes. The contaminated spectrum (absence of DNB) was also measured; the difference between it and the plotted spectrum is shown (×------×).

tion for $TMPD^+$ absorbance that was applied is also shown.

Actually, in the red, two spectra were determined, the true spectrum and a spectrum affected by an artefact. When no special precautions are taken, the data in the red contain a contribution from (Q_A^--dependent) fluorescence excited by the measuring beam. The spectral shape and amplitude of this artefact, as present under the general conditions of this study, are shown in Fig. 2B (broken line). The true spectrum was determined by adding dinitrobenzene (DNB), which is a fluorescence quencher [17,18]. By measuring the apparent extinction at varying quencher concentrations, a concentration was found (2 mM DNB) at which the fluorescence artefact was negligible.

The S2 minus S1 difference spectrum

The S2 − S1 spectra obtained in the blue, red and near-IR are shown in Fig. 3A, B and C. The applied correction for competition by the back reaction is also shown. It must be considered as uncertain, but is probably correct plus or minus 50%. The $Q_A^- - Q_A$ extinction coefficients used for the correction were apparent extinctions (true extinction plus artefact; see Fig. 2B). The correction applied is not indicated for the near-IR data: it was simply 6% of the original amplitude.

Flattening correction

To allow comparison of spectra obtained with different types of material, e.g., chloroplasts and smaller particles, a correction for flattening should be applied, i.e., for the diminution of absorbance changes caused by the mutual screening of the

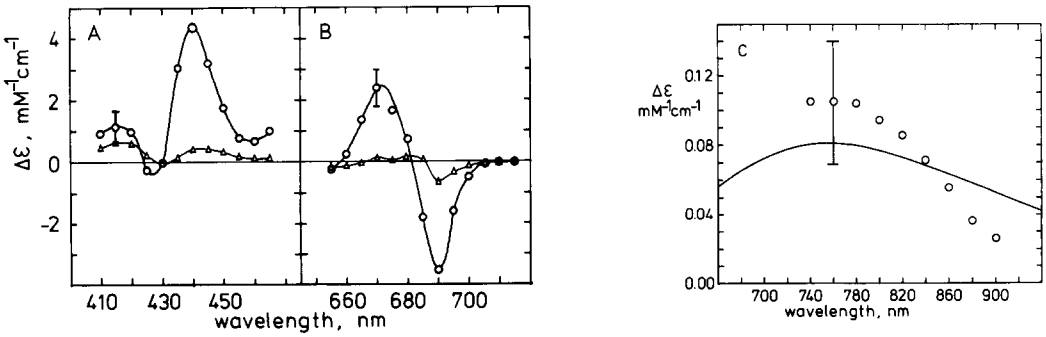

Fig. 3. Absorbance difference spectra of state S2 minus state S1 (○). Experimental conditions were the same as those described in Fig. 1C and D. Amplitudes of transients between 15 and 200 ms were plotted against wavelength after two corrections: for oxidation of TMPD (Fig. 2, thin line) and for simultaneous, competing oxidation of Q_A^- (△------△). The data were normalized against the absorbance change due to TMPD at 570 nm, taking $\Delta\varepsilon(TMPD^+ - TMPD, 570\ nm) = 11\ mM^{-1}\cdot cm^{-1}$ and $\Delta\varepsilon(S2-S1, 570\ nm) = 0$. To correct for particle flattening, the plotted data should be multiplied by the factors given in Fig. 2. The continuous line in C represents a typical theoretical curve for absorbance due to intervalence charge transfer of a mixed valence compound (see text).

pigments inside the particles in which they are contained [19]. According to Dekker et al. [4,20], only a small correction is necessary for the type of particle used in this study. The flattening factors derived from their results are given in Fig. 2. The amplitude of this correction is probably uncertain to at least ±50%. I should mention that using the same method as Dekker [20], i.e., comparing absorbance at 435 nm of particles suspended in aqueous medium or dissolved in organic medium, I did not succeed in obtaining a plausible value for the flattening amplitude with my own preparation: it came out unreasonably large, viz. about the same as that with chloroplasts. (A possible explanation of this result is that the preparation I used may not have been perfectly homogeneous and contained some specks of aggregated particles.)

Discussion

The Q_A^- minus Q_A difference spectrum

The $Q_A^- - Q_A$ spectrum obtained in the blue agrees well with reported spectra, which were measured with spinach [4], *Chlorella sorokiniana* [5] and *Synechococcus* [21]. It has been interpreted as due to an absorbance band of semiquinone with superimposed band shifts of pigments (pheophytin or chlorophyll); the most notable shift is a blue shift of a band centered near 425 nm [4,5,21]. The extinction values agree with those obtained by Dekker et al. [4], but only if one uses the same flattening factors as they did. This suggests that their correction factors do apply to the material that I used, and not the factors that I obtained myself (see above). Use of the latter factors would not greatly change the shape of the spectrum but it would about double the amplitude (not shown).

The spectrum in the red agrees rather poorly with reported spectra. The spectrum obtained with *Synechococcus* by Schatz and Van Gorkom [21] has a similar peak wavelength (approx. 682 nm) and peak amplitude (approx. 7 $mM^{-1} \cdot cm^{-1}$ [21]) as has the spectrum in Fig. 2B, but is quite different at its flanks (less bleaching at approx. 690 nm, more bleaching at approx. 660 nm, absence of the minor peak at approx. 672 nm). This spectrum was calculated from absorbance changes associated with the oxidation of Q_A^- by its endogenous acceptor, Q_B. However, the $Q_B^- - Q_B$ spectrum that was used in the calculations may have been flawed: unexpectedly, its red part was not composed purely of band shifts but showed a net increase of absorbance. The same $Q_B^- - Q_B$ spectrum was also used in calculating the $Z^+ - Z$ spectrum [21]. It is noteworthy that the resulting red part of this spectrum was again greatly dissimilar to that measured by another method, with spinach [4,21]. It seems dubious that these large differences can be ascribed to the difference in species. The spectrum that I obtained also agrees poorly with a spectrum obtained recently by Dekker [4], which was measured with the same material that I used. This spectrum does show the minor positive peak at approx. 672 nm, in addition to the major positive peak at approx. 682 nm and the negative peak at approx. 690 nm, but the estimated amplitude at 682 nm was only approx. 3 $mM^{-1} \cdot cm^{-1}$. The net change, integrated over frequency, was negative. This suggests that the spectrum was contaminated by a fluorescence artefact. My results agree better with an early spectrum of Van Gorkom [8] (see also Ref. 22); this was measured using an artificial donor acceptor that was at the same time a fluorescence quencher. However, Van Gorkom's spectrum and also a spectrum obtained by Klimov et al. [9] looked simpler than that of Fig. 2B: the changes observed seemed to be due predominantly to a blue shift of a band centered near 685 nm. This shift was interpreted by analogy with bacterial reaction centers [23] as a shift of pheophytin a [8,9]. However, there are difficulties with this interpretation. It is currently thought that the absorbance of the pheophytin that is located close to Q_A is centered near 680 nm [24]. Moreover, the bacterial pheophytin shifts in the opposite direction, toward higher wavelength; the bacterial centers show blue shifts in addition, but these are due to bacteriochlorophyll [23]. The analogy with bacterial centers is much improved by the spectrum of Fig. 2B. The spectrum clearly contains at least two components, a blue shift of one band and a red shift of a second, narrower band. It is likely that the blue-shifting band should be ascribed to chlorophyll and the red-shifting band to pheophytin, as in bacterial centers.

An attempt at simulation of the spectrum is

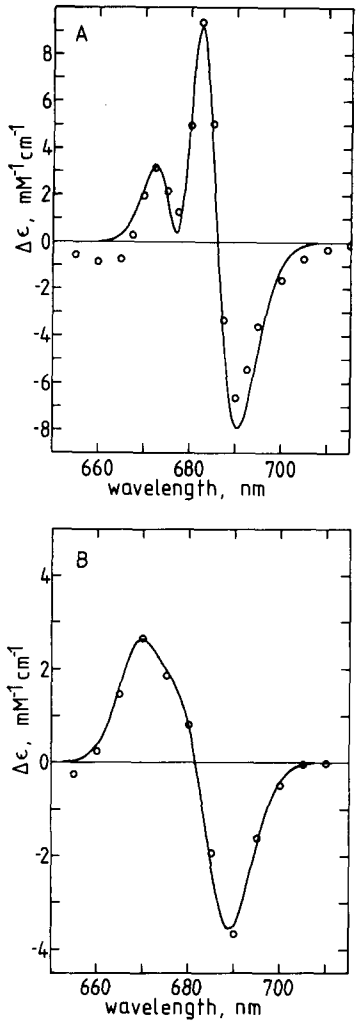

Fig. 4. Comparison of measured spectra with simulated spectra. The experimental data were taken from Figs. 2B and 3B, and were corrected for flattening. The simulated spectra are composed of shifts of absorbance bands that are assumed Gaussian on a frequency scale. See text for details.

illustrated in Fig. 4A. The simulation assumed a red shift due to a pheophytin band of oscillator strength 0.11 and a blue shift due to a chlorophyll band of oscillator strength 0.15. These are the approximate values of $Q_Y(0,0)$ bands of the two pigments in vitro (in medium of refractive index $n \approx 1.45$) [25]. The shape of the bands was assumed Gaussian on a frequency scale [25]. The fitted width of the bands was 70 cm^{-1} and 130 cm^{-1} Gaussian standard deviation (or 7.6 nm and 14.3 nm full width at half height), the initial peak positions 680.5 nm and 683 nm, and the shifts 0.3 nm (−0.8 meV) and −0.8 nm (2.1 meV), respectively. The fit is fair but not excellent, and it is unclear what assumptions are needed to improve it.

The S2 minus S1 difference spectrum in the visible

The obtained S2 − S1 difference spectrum in the blue agrees well with earlier spectra measured with particles from spinach [4] and a mutant strain of Chlorella sorokiniana [5,26]. It appears that the earlier spinach spectrum [4] may be slightly distorted in showing significant bleaching near 430 nm (extinction of about -1.5 $mM^{-1} \cdot cm^{-1}$), which is not observed in Fig. 3A, nor in Refs. 5 and 26. This distortion may have been caused by slight interference by PS I. Concerning the interpretation of the spectrum, it is likely that, as proposed [4,5], it is due to part to bandshifts of chlorophyll, notably a red shift of a band near 433 nm. However, the net absorbance change is clearly positive. This net absorbance is probably of similar origin as that which appears in the near ultraviolet, and which has been tentatively interpreted as due to charge-transfer bands of bound, oxidized manganese [4].

An S2 − S1 spectrum in the red has been obtained previously by Saygin and Witt [7], using small PS II particles from the blue-green alga *Synechococcus*. The spectrum reported was interpreted as resulting from the blue shift of a single chlorophyll band. The spectrum of Fig. 3B is similar to the spectrum reported, but is not identical to it, which is perhaps due to the difference in species. The amplitude of the spectrum reported was about 2-fold smaller than that of Fig. 3B, and the zero crossing point appeared to lie at approx. 676 nm while it lies at approx. 682 nm in Fig. 3B. The spectrum of Fig. 3B is poorly simulated by assuming a single band shift (not shown). This suggests that it contains more than one component, but the limited accuracy of the data does not allow a definitive conclusion on this. Fig. 4B illustrates that the data can be fitted excellently by assuming blue shifts of two chlorophyll $Q_Y(0,0)$ bands (Fig. 4B). The assumed oscillator strengths are 0.15 and 0.15. The fitted widths are 130 cm^{-1} and 120 cm^{-1} Gaussian standard deviation (or 14.3 and 12.8 full width at half height), initial

peak positions 683 nm and 673 nm, and shifts −0.32 nm (0.85 meV) and −0.15 nm (0.41 meV), respectively.

The near-infra red

S state-associated absorbance changes in the near-IR were first observed by Dismukes and Mathis [6]. These authors proposed that the S2 state might be related to the mixed valence Mn^{3+}/Mn^{4+} state of synthetic complexes of dimeric Mn, which similarly show absorbance in the near-IR. The theoretical shape of an intervalence charge-transfer band is indicated in Fig. 3C. A notable feature is its large width; the amplitude is difficult to predict. (Arbitrarily, absorbance was assumed to peak at approx. 780 nm. The curve was constructed using the following formula, taken from [27]: $\varepsilon = \varepsilon_0(h\nu/h\nu_0)\ \exp(-(h\nu_0 - h\nu)^2/4h\nu_0 kT)$, where $h\nu$ is the energy per light quantum and kT the thermal energy of a classical oscillator; this formula assumes that the dimer is symmetric, but allowance for several hundred meV of asymmetry does not change the shape a great deal.)

The results of Dismukes and Mathis seemed in good agreement with their hypothesis. However, the results shown in Fig. 3C rather weaken their case. At the peak of their spectrum, approx. 780 nm, the estimated extinction coefficient was 400–500 per $M \cdot cm^{-1}$. At this same wavelength, the extinction coefficient of Fig. 3C is about 4-times smaller, and the discrepancy between amplitudes is still larger toward higher wavelengths. The shape of the curve obtained does not fit the theoretical curve, but in view of the inprecision of the data this discrepancy could be due to chance. I am not absolutely certain that interference by PS I absorbance was insignificant in these data (although control experiments, not shown, indicated that this could not be responsible for more than approx. 1/3 of the amplitude). It is also uncertain to what extent the data of Fig. 3C (and those of Ref.6) are contaminated by scattering changes. It was pointed out by Dr. Van Gorkom (personal communication) that such contributions could be quite significant at the low levels of signal change that we encounter in the near-IR. The best way to examine this possibility critically is, of course, by appropriate experiments, which I have not done. Instead, I have tried to reach a conclusion by theoretical considerations, and these confirm that the contamination may indeed by serious. There is one clear reason to expect scattering changes. The formation of S2 is associated with a net absorbance increase in the visible and near-ultraviolet; this has consequences for scattering, which are analyzed in the Appendix. I have measured total scattering by the particles and obtained the result that, in the instrument that I used, the scattering analog of the extinction coefficient of the particles at 750 nm was about 400 per $cm \cdot mM^{-1}$ reaction center (assuming 1 reaction center per 250 chlorophyll). The changes observed, thus, amount to about 1/4000th of total scattering. The expected, estimated scattering increase is about 1/10000th (Appendix). This is smaller than what is observed, but only by a factor of about 2.5. Hence, and in view of the uncertainties in data and estimation, it seems quite possible that scattering changes are the dominant phenomenon in the near-IR. Perhaps there are real absorbance changes as well, but additional, careful measurements would be needed to prove this.

Appendix

Expected scattering increase in the near-IR due to increased absorbance in the near-ultraviolet and visible

The scattering efficiency (Q_{sca}) of a particle is a function of its size and of the dielectric permittivities (e_p and e_e, respectively) of it and its environment. The dependence on e is (see for example Ref. 28)

$$Q_{sca} \approx \frac{(e_p - e_e)^2}{(e_p + 2e_e)^2} \qquad \text{(A-1)}$$

It follows that when e_p changes by a small amount, the scattering change is approximately equal to

$$\Delta Q_{sca} = \frac{2\Delta e_p}{e_p - e_e} Q_{sca} \qquad \text{(A-2)}$$

The dielectric permittivity e is related to atomic and molecular properties by the equation (e.g., Ref. 29)

$$3\left(\frac{e-1}{e+2}\right) = \Sigma N\alpha \qquad \text{(A-3)}$$

where the terms $N\alpha$ are summed over all polarizable entities, $N(m^{-3})$ is the number of such entities per unit volume and α their 'polarizability'. When $\Sigma N\alpha$ increases by a small amount, it follows from Eqn. A-3 that e increases by approximately

$$\Delta e = \frac{(e+2)^2}{9}\Delta\Sigma N\alpha \qquad \text{(A-4)}$$

The polarizability can be related to absorbance by combining the formulas that relate α to oscillator strength and oscillator strength to absorbance. For frequencies, v_s, that lie well away from the range where the entities absorb, one has approx. (e.g., Ref. 29):

$$\alpha(\text{at } v_s) = 8.97 * 10^{-20}\frac{f}{v^2 - v_s^2} \qquad \text{(A-5)}$$

where f is the oscillator strength; the units of v and v_s are cm^{-1}. When Δe is small compared to e, and neglecting the slight dependence of e on wavelength, one may write (e.g., Ref. 25)

$$f = 2.60 * 10^{-15}\frac{1}{N_A}\frac{9n}{(e+2)^2}\int \varepsilon(v)\,dv \qquad \text{(A-6)}$$

where N_A is Avogadro's number, n is the refractive index, i.e., the square root of e, and ε ($M^{-1} \cdot cm^{-1}$) the extinction coefficient. From Eqns. A-5 and A-6 one obtains

$$\Delta\Sigma N\alpha(\text{at } v_s) = 2.33 * 10^{-4}\frac{N}{N_A}\frac{9n}{(e+2)^2}\int \frac{\Delta\varepsilon(v)\,dv}{v^2 - v_s^2} \qquad \text{(A-7)}$$

By combining Eqns. A-2, A-4 and A-7 one obtains finally

$$\frac{\Delta Q_{sca}}{Q_{sca}}(\text{at } v_s) = \frac{N}{N_A}\frac{4.67 * 10^{-4}}{e_p - e_e}n_p\int \frac{\Delta\varepsilon(v)\,dv}{v^2 - v_s^2} \qquad \text{(A-8)}$$

The units are: N/N_A (the reciprocal molar particle volume) in m^{-3}, v in cm^{-1}, ε in $M^{-1} \cdot cm^{-1}$.

Evaluation

The molecular weight of oxygen evolving particles from *Synechococcus* was estimated as approx. 300000 [30]. Starting from this value, a reasonable guess for the 'BBY' (Bertold, Babcock and Yocum) preparation used in this work is that the weight per reaction center is approx. 900000. The *Synechococcus* particles contain approx. 50 chlorophyll [30], but the BBY particles contain approx. 250 chlorophyll [4,11]. The additional chlorophyll, together with its associated protein (estimated as 1700 g per mol chlorophyll [31]), adds approx. 500000 per reaction center. The *Synechococcus* particles contain approx. 45 kDa of non-pigmentous, polar lipids [30]. I assumed that the BBY preparation contains an additional approx. 100 kDa of polar lipids per reaction center (which gives a total of approx. 0.65 g polar lipids per g chlorophyll, which is approx. 1/4 that of thylakoid membranes [32]). Using 900 kDa and density approx. 1.1, the reciprocal volume per mol reaction center is thus estimated as approx. 1.2 m^{-3}.

The dielectric permittivity of the medium, a solution of approx. 0.4 M of sucrose, is approx. 1.83. A reasonable guess for the composite dielectric permittivity of the particles is 2.4. This is the approximate literature value for protein [33]. The literature value for lipid is slightly smaller, 2.2 [33]. The value for pigmentous lipids must be higher than 2.2. With e_p set at 2.4, n_p is set at 1.55.

The last part of Eqn. A-8, the integral, can be estimated using Fig. 7 of Ref. 4. Integrating between 240 nm and 500 nm, for scattering at 750 nm, i.e., $v_s = 13300\ cm^{-1}$, I obtained a value of approx. 0.094. (I ignored contributions by the band shift in the red; they are minor). Naturally, to estimate in a correct manner, the integration should have been carried out over the entire range where the absorbance changes, but in practice this cannot be done because $\Delta\varepsilon$ below 240 nm is currently unknown. More likely than not, however, the contribution of the range below 240 nm is not all that large. Suppose, conservatively, and for the purpose of these calculations only, that the $\Delta\varepsilon$ below 240 nm is entirely negative (even although Fig. 7 of Ref. 4 suggests that this is not true) and that it consists of the bleaching of a narrow band located at 210 nm. I suppose that, despite the loss of an electron, it is reasonable to employ the assumption that ε changes overall in such a way that the total oscillator strength remains unchanged. The negative contribution to

the integral of Eqn. A-8 must, thus, be smaller than the positive contribution, because of their different weighting by the factor $1/(v^2 - v_s^2)$; I calculated that, with the specified assumptions, it is approx. 33% of the positive contribution. If the compensating bleaching is centered at a wavelength lower than 210 nm, the correction will be smaller. We thus obtain a corrected, minimal value of approx. 0.063.

Using the above values in Eqn. A–8, one obtains $\Delta Q_{sca}/Q_{sca}$ = approx. $1 \cdot 10^{-4}$.

References

1 Crofts, A.R. and Wraight, C.A. (1983) Biochim. Biophys. Acta 726, 149–185.
2 Pulles, M.P.J., Van Gorkom, H.J. and Willemsen, J.G. (1976) Biochim. Biophys. Acta 449, 536–540.
3 Velthuys, B.R. (1981) in Photosynthesis II (Akoyunoglou, G., ed.), pp. 75–85, Balaban International Science Services, Philadelphia.
4 Dekker, J.P., Van Gorkom, H.J., Brok, M. and Ouwehand, L. (1984) Biochim. Biophys. Acta 764, 301–309
5 Lavergne, J. (1984) FEBS Lett. 9–14.
6 Dismukes, G.C. and Mathis, P. (1984) FEBS Lett. 178, 51–54.
7 Saygin, O. and Witt, H.T. (1985) FEBS Lett. 187, 224–226.
8 Van Gorkom, H.J. (1974) Biochim. Biophys. Acta 347, 439–442.
9 Klimov, V.V., Klevanik, A.V., Shuvalov, V.A. and Krasnovsky, A.A. (1977) FEBS Lett. 82, 183–186.
10 Hiyama, T. and Ke, B. (1972) Biochim. Biophys. Acta 267, 160–171.
11 Berthold, D.A., Babcock, G.T. and Yocum, C.F. (1981) FEBS Lett. 134, 231–234.
12 Forster, V., Hong, Y. and Junge, W. (1981) Biochim. Biophys. Acta 638, 141–152.
13 Velthuys, B.R. (1983) in The Oxygen-Evolving System of Photosynthesis (Inoue, Y., Crofts, A.R., Govindjee, Murata, N., Renger, G. and Satoh, K., eds.), pp. 83–90, Academic Press, Tokyo.
14 Tamura, N., Radmer, R., Lantz, S., Cammarata, K. and Cheniae, G. (1986) Biochim. Biophys. Acta 369–379.
15 Bennoun, P. (1978) Biochim. Biophys. Acta 216, 357–363.
16 Agalidis, I. and Velthuys, B.R. (1986) FEBS Lett. 197, 263–266.
17 Amesz, J. and Fork, D.C. (1967) Biochim. Biophys. Acta 143, 97–107.
18 Etienne, A.L. and Lavergne, J. (1972) Biochim. Biophys. Acta 283, 268–278.
19 Duysens, L.N.M. (1956) Biochim. Biophys. Acta 19, 1–12.
20 Dekker, J.P. (1985) Thesis, University of Leiden, Leiden.
21 Schatz, G.H. and van Gorkom, H.J. (1985) Biochim. Biophys. Acta 810, 283–294.
22 Van Gorkom, H.J. (1976) Thesis, University of Leiden, Leiden.
23 Clayton, R.K. and Straley, S.C. (1972) Biophys. J. 12, 1221–1234.
24 Ganago, I.B., Klimov, V.V., Ganago, A.O., Shuvalov, A. and Erokhin, Y.E. (1982) FEBS Lett. 127–130.
25 Shipman, L.L. (1977) Photochem. Photobiol. 26, 287–292.
26 Lavergne, J. (1987) Biochim. Biophys. Acta 894, 91–107.
27 Hush, N.S. (1967) Progr. Inorg. Chem. 8, 391–444.
28 Garab, G.I., Paillotin, G. and Joliot, P. (1979) Biochim. Biophys. Acta 445–453.
29 Feynman, R.P., Leighton, R.B. and Sands (1964) The Feynman Lectures on Physics, Vol. 2, Chapter 32, Addison-Wesley, Reading.
30 Ohno, T., Satoh, K. and Katoh, S. (1986) Biochim. Biophys. Acta 852, 1–8.
31 Burke, J.J., Ditto, C.L. and Arntzen, C.J. (1978) Arch. Biochem. Biophys. 187, 252–263.
32 Lichtenthaler, H.K. and Park, R.B. (1963) Nature 198, 1070–1072.
33 Duniec, J.T. and Thorne, S.W. (1977) J. Bioenerg. Biomembr. 9, 223–235.